ARTICLES

Journal of Semiconductors
(2020) 41, 072905
doi: 10.1088/1674-4926/41/7/072905

Gate-regulated transition temperatures for electron hopping behaviours in silicon junctionless nanowire transistors

Xinyu Wu[1, 2], Weihua Han[1, 2, †], Xiaosong Zhao[1, 2], Yangyan Guo[1, 2], Xiaodi Zhang[1, 2], and Fuhua Yang[1, 2, 3, †]

[1]School of Microelectronics, University of Chinese Academy of Sciences, Beijing 100049, China

[2]Engineering Research Center for Semiconductor Integrated Technology, Institute of Semiconductors, Chinese Academy of Sciences, Beijing 100083, China

[3]State Key Laboratory for Superlattices and Microstructures, Institute of Semiconductors, Chinese Academy of Sciences, Beijing 100083, China

Abstract: We investigate gate-regulated transition temperatures for electron hopping behaviours through discrete ionized dopant atoms in silicon junctionless nanowire transistors. We demonstrate that the localization length of the wave function in the spatial distribution is able to be manipulated by the gate electric field. The transition temperatures regulated as the function of the localization length and the density of states near the Fermi energy level allow us to understand the electron hopping behaviours under the influence of thermal activation energy and Coulomb interaction energy. This is useful for future quantum information processing by single dopant atoms in silicon.

Key words: silicon junctionless nanowire transistor; discrete dopant atoms; gate regulation; transition temperatures

Citation: X Y Wu, W H Han, X S Zhao, Y Y Guo, X D Zhang, and F H Yang, Gate-regulated transition temperatures for electron hopping behaviours in silicon junctionless nanowire transistors[J]. *J. Semicond.*, 2020, 41(7), 072905. http://doi.org/10.1088/1674-4926/41/7/072905

1. Introduction

Dopant atoms may draw more attention when they are used as a functional unit of ultra-small electronic devices instead of just providing carriers[1–3]. For example, new applications that require the discreteness of dopants, such as dopant-based spin qubits in the area of quantum computation[4, 5] or single atom transistors[6], focus more on the advances toward observing, precise positioning and manipulating dopant atoms[7–10]. Owing to the emergence of high-pure semiconductor materials and the extreme downscaling of devices, discrete dopants have started to play an important role in most device transport properties[11, 12]. In the last few years, the junctionless nanowire transistor (JNT) with uniform doping is considered to be a promising candidate to investigate quantum transport through dopant atoms due to its unique bulk conduction regulated by gate electric field[13–15].

Electron transport in the discrete dopant atomic system may be dominated by thermally assisted hopping between the dopants rather than by resonant tunnelling between source and drain. At higher temperatures, electrons can hop between the neighbouring dopants when they receive enough energy from a phonon, following the nearest-neighbour hopping (NNH) mechanism. The conductance in this case is given by $G = A\exp(-E_a/k_BT)$, where A is constant, k_B is the Boltzmann constant, and E_a is the activation energy. At lower temperatures, the conductance is weakly temperature-dependent because variable range hopping (VRH) with lower activation energy is dominated. In a regime of VRH, the general form of temperature-dependent conductance is given by

$$G = G_0\exp(-T_0/T)^x. \tag{1}$$

The conductive channel in silicon junctionless nanowire transistor expands from the middle of the nanowire to the surrounding by adjusting the gate voltage. Once the junctionless nanowire transistor is turned on, the channel of electron transport can be seen as a quasi three-dimensional (3D) system. In the 3D case, the conductance follows the Mott law (M-VRH)[16] with

$$x = 1/4,\ T_0 \equiv T_M = 21/g\left(E_F\right)a_M^3, \tag{2}$$

where $g\left(E_F\right)$ is the constant density of state at the Fermi level and a is the localization length. If the Coulomb interaction between the charged sites is not negligible at low temperature, the conductance follows Efros-Shklovskii law (ES-VRH)[17, 18] with

$$x = 1/2,\ T_0 \equiv T_{ES} = 2.8e^2/\kappa a_{ES},\ \kappa = 4\pi\varepsilon_0\varepsilon_r, \tag{3}$$

where e is the electron charge, ε_r is the relative permittivity and a_{ES} is the localization length in a regime of ES-VRH. The transition of electron hopping behaviours in the JNT, which can be well explained by Mott and Efros-Shklovskii (ES) formalism, has been studied in our previous work[19, 20]. In this work, we investigate gate-regulated transition temperatures of electron hopping behaviours through discrete dopant atoms. The energy range of accessible hopping sites in NNH is greater than the average energy in dopant band and the localization length in M-VRH is less than the mean distance between the dopant atoms, resulting in a relatively stable transition temperature T_A from M-VRH to NNH. The increasing transition

Correspondence to: W H Han, weihua@semi.ac.cn; F H Yang, fhyang@semi.ac.cn

Received 6 MARCH 2020; Revised 2 APRIL 2020.

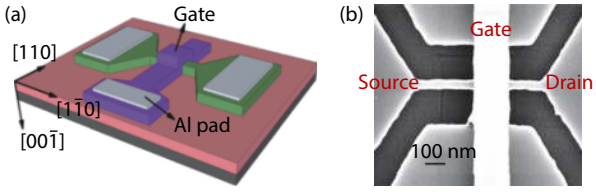

Fig. 1. (Color online) (a) Schematic structure of the silicon JNT. (b) Top-view SEM images of the silicon JNT after gate formation.

temperature T_C from ES-VRH to M-VRH is due to the longer localization length which is more easily regulated by gate voltage. The dependence of transition temperature T_C on gate voltage also implies a competition between the activation energy and the Coulomb interaction, which extends the knowledge of electron hopping.

2. Device fabrication and characterization

Fig. 1(a) shows a schematic of the devices fabricated on a (100)-oriented silicon-on-insulator (SOI) wafer with top silicon thickness of 55 nm and buried oxide layer of 145 nm. The SOI wafer with a 17-nm thermal oxidation layer was uniformly implanted by 33 keV phosphorus ions at a dose of 2×10^{12} cm^{-2}, followed by rapid annealing to activate dopant atoms. The silicon nanowire was defined by electron beam lithography (EBL) and reactive ion etching (RIE), followed by thermal oxidation at 900 °C to form a sacrificial oxidation layer. Next, this sacrificial oxidation layer was removed by buffered oxide etcher (BOE) to smooth the surface and further reduce the dimension of silicon nanowire. After formation of 22-nm-thick gate oxidation layer around the nanowire at 900 °C in dry oxygen, 200-nm-thick boron-doped polycrystalline silicon was deposited on the devices by low-pressure chemical vapor deposition (LPCVD). Subsequently, the polycrystalline silicon gate of 280 nm was patterned by electron beam lithography and dry etching, followed by deposition of 200 nm SiO_2 for passivation and fabrication of the source, drain and gate electrodes. The width of 60 nm for Si/SiO_2 core-shell nanowire measured by scanning electron microscope (SEM) is shown in Fig. 1(b). According to the consumption of top silicon layer by thermal oxidation in all directions, the cross-section of the silicon core is estimated to be 16×28 nm^2. The electrical characteristics were measured by Agilent B1500 semiconductor parameter analyzer, and the devices were placed in a vacuum chamber which can be cooled down to 6 K with the help of a Lakershore-340 temperature controller.

3. Results and discussion

Fig. 2 shows drain current–gate voltage (I_{ds}–V_g) characteristics (upper part) and corresponding transconductance g_m–V_g characteristics (lower part) of JNT at the drain–source bias V_{ds} = 10 mV by varying temperature. Clearly, a series of drain-current oscillatory peaks and steps are observed below the temperature of 75 K, and these current features gradually disappear with increasing temperature due to thermal energy broadening around Fermi level. The drain current at low temperature, which evolves from oscillatory peaks to current steps with the gate voltage, reflects that electron transport in dopant-levels gradually transfers into one-dimensional transport in conduction sub-bands. Similar features have

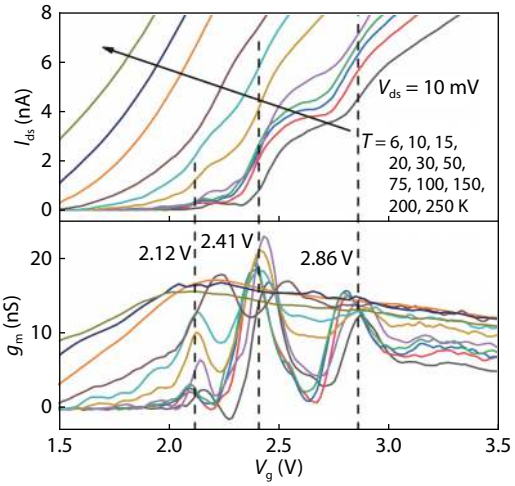

Fig. 2. (Color online) Drain current I_{ds} versus gate voltage V_g with V_{ds} = 10 mV at different temperatures (upper part) and corresponding transconductance g_m–V_g curves (lower part).

also been observed in other devices that have been fabricated in the same way. According to the corresponding curves of the transconductance g_m as a function of gate voltage V_g (i.e., $g_m = \partial I_{ds}/\partial V_g$) in the lower part, we can identify three groups of peaks which locate at the gate voltage of about 2.12, 2.41, and 2.86 V, respectively. The positions of peaks at different temperatures in each group are slightly different, possibly due to the interface defects at the Si/SiO_2 interface and the electron density from the ionized dopants[21]. These transconductance peaks may originate from dopant-induced quantum dots and discrete sub-bands in the conduction band.

To distinguish the three groups of transconductance peaks precisely, we measured the energy barrier between source and drain extracted from the thermally activated current at temperatures above 150 K. As shown in Fig. 3(a), the barrier height gradually decreases with gate voltage, which is associated with lower activation energy at larger electrical field. The gate voltage at 2.40 V can be determined by linear extrapolation of the curve to zero barrier height, showing that the conduction band edge E_c reaches the Fermi level E_F of the source. It can be also observed that the position of gate voltage 2.40 V corresponds to a demarcation line between the first group of transconductance peaks and the other two groups in the inset of Fig. 3(a). As a result, the first group of transconductance peaks in Fig. 2 comes from discrete dopant-levels below the conduction edge. Then, one-dimensional transport of electrons occurs in the conduction sub-bands with the increase of gate voltage, resulting in the second and third groups of transconductance peaks.

We can identify new four groups of peaks marked by cross in Fig. 3(b) through locally amplifying the transconductance g_m–V_g curves before 2.40 V. Since the gate-voltage spacing of those peaks is small and the positions of them are basically the same at different temperatures, those transconductance peaks can not originate from the surface roughness of the silicon nanowire. It is reported that dopants in the conductive channel have an effect on electron transport when the JNT is just turned on[22–24]. The ionized dopant atoms in local nano-space can work as quantum dots, containing one-electron neutral D^0 state and two-electrons charged

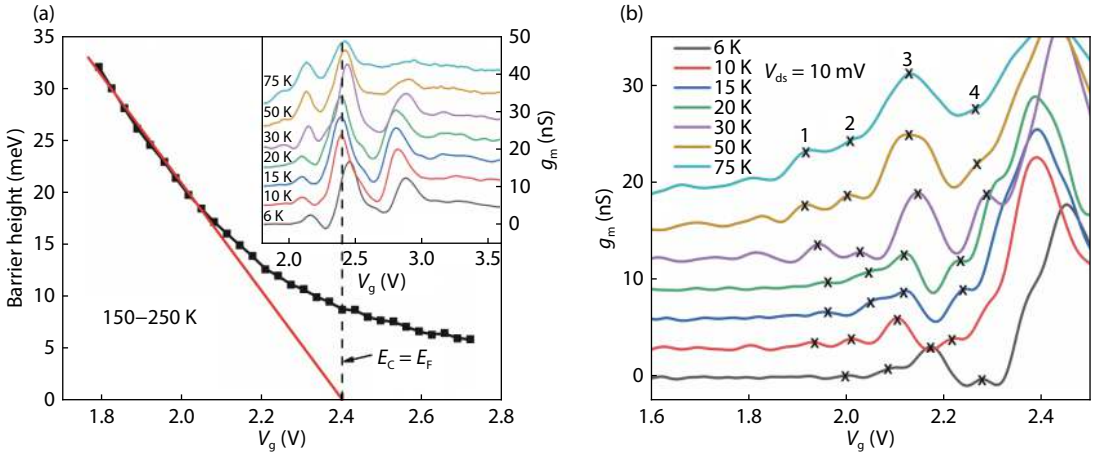

Fig. 3. (Color online) (a) Barrier height of the device channel is extracted by fitting the thermally activated current. The conduction band edge E_C reaches the Fermi level E_F at 2.40 V. Inset: transconductance g_m–V_g curves at low temperature. (b) Locally amplified transconductance g_m–V_g curves before gate voltage 2.40 V, which are successively shifted for clarify.

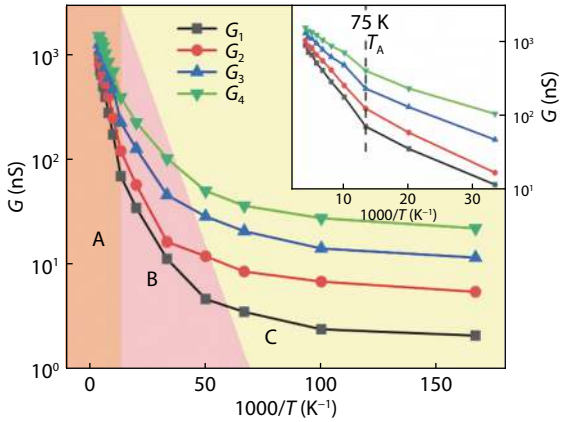

Fig. 4. (Color online) Arrhenius plots of the conductance G_1, G_2, G_3, and G_4 for each group. The inset: close-up of the curves around 75 K.

D^- state. The average gate voltage spacing ΔV_{gs} between peaks 1 and 3 (peaks 2 and 4) in Fig. 3(b) is estimated to be 0.18 V (0.21 V), and the deduced dopant/gate capacitance $C_g = e/\Delta V_{gs} = 0.89$ aF (0.76 aF) corresponds to a dopant with 2.09 nm (1.78 nm) radius. This radius agrees well with the Bohr radius of a donor in silicon nanowire. Therefore, the four groups of peaks can be considered as an indication of electron transport through the D^0 and D^- states of the donors. At high doping concentration, a lower Hubbard band and an upper Hubbard band are formed respectively under the coupling of one-electron neutral state (D^0) and two-electron charged state (D^-). In this case, electron transport is due to the Hubbard band which is different from the mechanism that we discussed in this study. According to the implantation dose, the doping concentration N_D is calculated to be 1×10^{17} cm^{-3}. Then, the mean distance between the dopant atoms is estimated to be $d = (4\pi N_D/3)^{-1/3} \approx 13.4$ nm, which is more than twice the Bohr radius of phosphorus atoms in silicon. It can be concluded that those dopant atoms are in a discrete state[25]. In this case, electron transport is dominated by thermally activated hopping.

To obtain a better insight into the electron hopping mechanism, we experimentally extracted the conductance values at the position of transconductance peaks in each group, and those unrecognizable peaks at high temperatures are determined by the method of energy level alignment. Fig. 4 shows the Arrhenius plots (G versus $1/T$) of temperature-dependent conductance G_1, G_2, G_3, and G_4, respectively at the transconductance peaks of different gate voltages under the bias $V_{ds} = 10$ mV. Three regions (i.e., A, B, and C) in the Arrhenius plots of conductance correspond to NNH, M-VRH and ES-VRH. The transition temperature T_A from NNH to M-VRH is a critical point at which the hopping distance in M-VRH is supposed to be equivalent to the mean distance between neighbouring dopant atoms. The expression of T_A is given by $T_A = 9a_M/8\pi g_0 k_B d^4$, a_M being the localization length in a regime of M-VRH, g_0 the constant density of states at the Fermi level and d the mean distance between the dopant atoms. The transition temperature T_C from M-VRH to ES-VRH is another critical point at which the activation energy E_a is as large as the Coulomb interaction energy Δ, i.e., $E_a = \Delta$. The expression of T_C is given by $T_C = e^4 a g_0/(4\pi\varepsilon_0\varepsilon_r)^2 k_B$, where a_{ES} is the localization length in a regime of ES-VRH, e is the electron charge and ε_r is the relative permittivity. The detailed calculation methods of transition temperatures have been reported in our previous work[20]. Through conductance linear fitting in different temperature region, we obtain the transition temperature T_A of 78, 80, 79, and 81 K respectively for the G_1, G_2, G_3, and G_4 curves in Fig. 4, which is consistent with the experimental value 75 K. Using the constant density of states g_0 in M-VRH regime and the relative permittivity ε_r for silicon material, we get the transition temperature T_C of 18, 27, 38, and 46 K, which is also consistent with the experimental phenomenon in Fig. 4. According to the conductance values at the corresponding positions of transconductance valleys in Fig. 3(b), we further calculated the transition temperatures T_A to be 79, 76, 76, and 78 K and T_C to be 22, 30, 41, and 53 K.

The gate-voltage dependence of the transition temperatures is provided in the Fig. 5(a). It can be found that T_A is relatively stable for the transconductance peak and valley positions, while T_C increases with the increase of gate voltage. The difference between T_A and T_C is associated with the density of state g_0 and the localization length, as shown in Fig. 5(b). According to the Eqs. (2) and (3), the characteristic

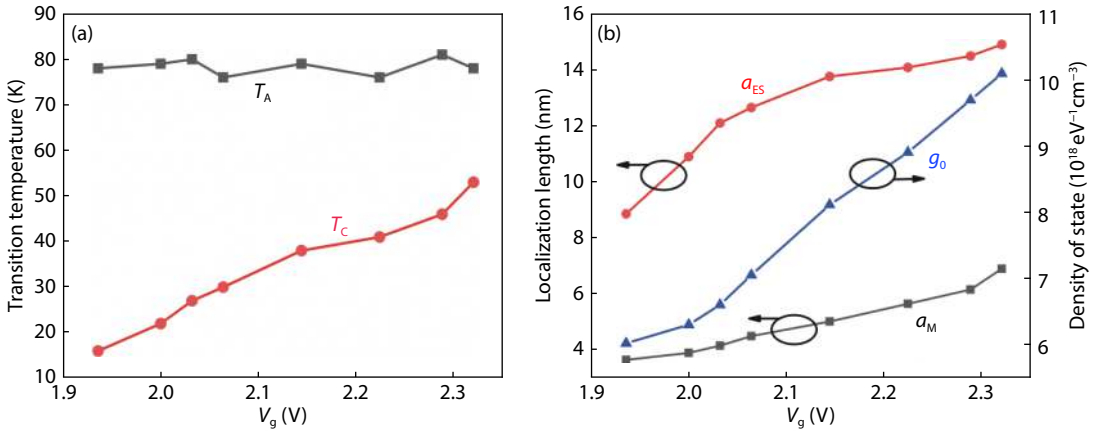

Fig. 5. (Color online) (a) The gate-voltage regulated transition temperature T_A and T_C. (b) The gate-voltage dependence of the density of state and the localization length.

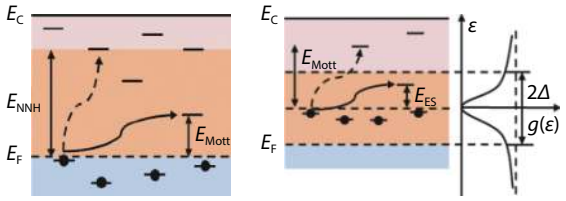

Fig. 6. (Color online) The behaviour of electron hopping (a) from M-VRH to NNH in and (b) from ES-VRH to M-VRH in.

temperatures T_M and T_{ES} can be derived from the slopes of the $\ln G - T^{-1/4}$ and $\ln G - T^{-1/2}$ plots, respectively. Then the localization length a_M and a_{ES}, which correspond to M-VRH and ES-VRH respectively, are extracted from T_M and T_{ES}. Fig. 5(b) indicates that both the density of state g_0 and the localization length a_M and a_{ES} increase with the increasing gate voltages, which allow more dopant atoms to work as quantum dots with lower barriers in a wider channel. The spatial extent of electron wave function from those dopant sites is also enhanced by the enhanced gate electric field.

To understand the stable transition temperature T_A at which electron hopping behaviours from M-VRH to NNH occurs, in Fig. 6(a) we describe the transition of hopping behaviours. Mott's model has pointed out that electrons localized close to the Fermi level could hop from one localized site to another with the lowest activation energy E_{Mott} by variable ranges. However, the activation energy E_{NNH} at higher temperatures is large enough for electron hopping between any nearest neighbouring sites, and the increasing gate voltage only contributes to the number of electrons capable of hopping in those sites. We also notice in Fig. 5(b) that the localization length a_M in M-VRH is much less than the mean distance d between the dopant atoms, i.e. $d/a_M \gg 1$. In this case, the coupling of electron wave function between nearest neighbour dopant atoms is very weak although the localization length a_M increases with the increasing gate voltages in Fig. 5(b). Therefore, the stable transition temperature T_A should attribute to large activation energy and small localization length in the regime of M-VRH.

The gate-dependent transition temperature T_C is regulated by the density of states and the localization length a_{ES} in ES-VRH. At lower temperatures, electrons would choose further localized states to hop due to the low activation energy E_{ES}, which is not enough to overcome the Coulomb interaction energy $\Delta = e^2/4\pi\varepsilon_0\varepsilon_r r$. With the increase of gate voltage, the number of states for electron hopping increases, resulting in the decrease of the average hopping distance r_{ES} of electrons, and the Coulomb interaction energy, $\Delta = e^2/4\pi\varepsilon_0\varepsilon_r r_{ES}$, will be remarkably enhanced due to the shorter distance r_{ES} between the charged dopant atoms. To overcome this stronger Coulomb interaction energy, a larger activation energy is required when the process from ES-VRH to M-VRH occurs. In addition, the localization length a_{ES} in ES-VRH is comparable or even larger than the mean distance d between the dopant atoms in Fig. 5(b). In this case, the localization length a_{ES} is more easily regulated by the gate's electrical field and its effect on electron hopping begins to show up. Therefore, higher transition temperature T_C is necessary to satisfy with the condition of $E_a = \Delta$ with the increase of gate voltages. According to the expression of electron hopping distance in ES-VRH given by $r_{ES} = \left[e^2 a_{ES}/2(4\pi\varepsilon_0\varepsilon_r)k_B T\right]^{1/2}$[20], the increasing localization length a_{ES} also requires a higher transition temperature T_C to keep the equation in balance because the electron hopping distance r_{ES} decreases with the increase of gate voltage. Under the influence of electrical field, the equilibrium of activation energy and Coulomb interaction energy at transition temperature T_C is broken. The dependence of transition temperature on gate voltage represents a new competition between them.

4. Conclusion

In conclusion, we investigate gate-regulated transition temperatures of electron hopping behaviours in silicon junctionless nanowire transistor. The experimental data of temperature-dependent conductance illustrated by the Arrhenius plots is consistent with the theoretical model, showing that the electron hopping is ES-VRH, M-VRH and NNH with the increase of temperature. The transition temperature T_A is relatively stable and mainly depends on the mean distance between the dopant atoms. In contrast, the transition temperature T_C can be regulated by gate electrical field due to the longer localization length in the case of ES-VRH. The role of dopant atoms used as functional units becomes more and more important in ultra-small devices and the study on elec-

tron hopping by dopant atoms is of great significance to the development of those atomic-scale silicon transistors.

Acknowledgements

The authors acknowledge Dr. Hao Wang, Dr. Liuhong Ma and Mr. Xiaoming Li for their helps in device fabrication. This work was supported by the National Key R&D Program of China (Grant No.2016YFA0200503).

References

[1] Koenraad P M, Flatté M E. Single dopants in semiconductors. Nat Mater, 2011, 10, 91
[2] Lansbergen G P, Rahman R, Wellard C J, et al. Gate-induced quantum-confinement transition of a single dopant atom in a silicon FinFET. Nat Phys, 2008, 4, 656
[3] Fresch B, Bocquel J, Rogge S, et al. A probabilistic finite state logic machine realized experimentally on a single dopant atom. Nano Lett, 2017, 17, 1846
[4] Hollenberg L C L, Dzurak A, Wellard C J, et al. Charged-based quantum computing using single donors in semiconductors. Phys Rev B, 2004, 69, 113301
[5] Ladd T D, Jelezko F, Laflamme R, et al. Quantum computers. Nature, 2010, 464, 45
[6] Fuechsle M, Miwa J A, Mahapatra S, et al. A single-atom transistor. Nat Nanotechnol, 2012, 7, 242
[7] Prati E, Hori M, Guagliardo F, et al. Anderson–Mott transition in arrays of a few dopant atoms in a silicon transistor. Nat Nanotechnol, 2012, 7, 443
[8] Dagesyan S A, Shorokhov V V, Presnov D E, et al. Sequential reduction of the silicon single-electron transistor structure to atomic scale. Nanotechnology, 2017, 28, 225304
[9] Ryu H, Lee S, Fuechsle M, et al. A tight-binding study of single-atom transistors. Small, 2015, 3, 374
[10] Tabe M, Moraru D, Ligowski M, et al. Single-electron transport through single dopants in a dopant-rich environment. Phys Rev Lett, 2010, 105, 016803
[11] Li Y, Yu S, Hwang J, et al. discrete dopant fluctuations in 20-nm/15-nm-gate planar CMOS. IEEE Trans Electron Devices, 2008, 55(6), 1449
[12] Akhavan N D, Ferain I, Yu R, et al. Influence of discrete dopant on quantum transport in silicon nanowire transistors. Solid-State Electron, 2012, 70, 92
[13] Colinge J P, Lee C W, Afzalian A, et al. Nanowire transistors without junctions. Nat Nanotechnol, 2010, 5, 225
[14] Ueda A, Luisier M, Sano N. Enhanced impurity-limited mobility in ultra-scaled Si nanowire junctionless field-effect transistors. Appl Phys Lett, 2015, 107, 253501
[15] Uddin W, Georgiev Y M, Maity S, et al. Dopant induced single electron tunneling within the sub-bands of single silicon NW tri-gate junctionless n-MOSFET. J Phys D, 2017, 50, 365104
[16] Mott N F. Conduction in non-crystalline materials. New York: Clarendon Press, 1987
[17] Efros A L, Shklovskii B I. Electronic properties of doped semiconductors. Berlin: Springer- Verlag, 1984
[18] Efros A L, Shklovskii B I. Coulomb gap and low-temperature conductivity of disordered systems. J Phy C, 1975, 8, 49
[19] Wang H, Han W, Li X, et al. Low-temperature study of array of dopant atoms on transport behaviors in silicon junctionless nanowire transistor. J Appl Phys, 2014, 116, 124505
[20] Guo Y Y, Han W H, Zhao X S, et al. Observation of hopping transitions for delocalized electrons by temperature-dependent conductance in silicon junctionless nanowire transistors. Chin Phys B, 2019, 28, 107303
[21] Wang H, Han W, Ma L, et al. Current-voltage spectroscopy of dopant-induced quantum-dots in heavily n-doped junctionless nanowire transistors. Appl Phys Lett, 2014, 104, 133509
[22] Büch H, Fuechsle M, Baker W, et al. Quantum dot spectroscopy using a single phosphorus donor. Phys Rev B, 2015, 92, 235309
[23] Tettamanzi G C, Hile S J, House M G, et al. Probing the quantum states of a single atom transistor at microwave frequencies. ACS Nano, 2016, 11, 2444
[24] Tyszka K, Moraru D, Samanta A, et al. Comparative study of donor-induced quantum dots in Si nano-channels by singleelectron transport characterization and Kelvin probe force microscopy. J Appl Phys, 2015, 117, 244307
[25] Moraru D, Samanta A, Tyszka K, et al. Tunneling in systems of coupled dopant-atoms in silicon nano-devices. Nanoscale Res Lett, 2015, 10, 372